Quaternary Geochronology 38 (2017) 1–12

Contents lists available at ScienceDirect

Quaternary Geochronology

journal homepage: www.elsevier.com/locate/quageo

Research paper

# A new approach for constraining the magnitude of initial disequilibrium in Quaternary zircons by coupled uranium and thorium decay series dating

Shuhei Sakata [a, *], Shinsuke Hirakawa [b], Hideki Iwano [c], Tohru Danhara [c], Marcel Guillong [d], Takafumi Hirata [e]

[a] Department of Chemistry, Faculty of Science, Gakushuin University, Mejiro 1-5-1, Toshima-ku, Tokyo 171-8588, Japan
[b] Laboratory for Planetary Sciences, Kyoto University, Kitashirakawa Oiwakecho, Sakyo-ku, Kyoto 606-8502, Japan
[c] Kyoto Fission-Track Co., Ltd., Minamitajiri-cho 44-4, Omiya, Kita-ku, Kyoto 603-8832, Japan
[d] Institut Für Geochemie und Petrologie, ETH Zürich, NW D 77.2, Clausiusstrasse 25, 8092 Zürich, Switzerland
[e] Geochemical Research Center, The University of Tokyo, Hongo 7-3-1, Bunkyo-ku, Tokyo 113-0033, Japan

ARTICLE INFO

*Article history:*
Received 15 October 2014
Received in revised form
28 October 2016
Accepted 15 November 2016
Available online 17 November 2016

*Keywords:*
Zircon
U-Th-Pb dating
LA-ICP-MS
Melt disequilibrium
Elemental partitioning

ABSTRACT

We have measured $^{238}U$–$^{206}Pb$, $^{235}U$–$^{207}Pb$, and $^{232}Th$–$^{208}Pb$ ages on Quaternary zircons by laser ablation, single-collector, magnetic sector inductively coupled plasma mass spectrometry (LA-ICP-MS). To obtain reliable ages for Quaternary zircons, corrections for initial disequilibrium associated with deficits and excesses of both $^{230}Th$ and $^{231}Pa$ relative to secular equilibrium resulting from differential partitioning during zircon crystallization or source melting must be made. In contrast, the $^{232}Th$–$^{208}Pb$ decay system is clearly advantageous for samples affected by disequilibrium because the $^{232}Th$ decay system lacks long-lived intermediate daughter isotopes. Conventionally, the initial disequilibrium for the $^{238}U$ and $^{235}U$ decay series has been determined by the distribution ratio between the melt and zircon (i.e., $f_{Th/U} = (Th/U)_{Zircon}/(Th/U)_{Melt}$ and $f_{Pa/U} = (Pa/U)_{Zircon}/(Pa/U)_{Melt}$). In our study, these correction factors were determined from comparison of the measured $^{238}U$–$^{206}Pb$ and $^{235}U$–$^{207}Pb$ ages with $^{232}Th$–$^{208}Pb$ ages obtained for three zircons of known eruption and, in some cases, zircon crystallization ages (Kirigamine Rhyolite, Bishop Tuff, and Toga Pumice). The resulting correction factors are $f_{Th/U} = 0.19 \pm 0.14$ and $f_{Pa/U} = 3.66 \pm 0.89$ (Kirigamine Rhyolite), $f_{Th/U} = 0.24 \pm 0.20$ and $f_{Pa/U} = 3.1 \pm 1.2$ (Bishop Tuff), and $f_{Th/U} = 0.28 \pm 0.17$ and $f_{Pa/U} = 3.04 \pm 0.99$ (Toga Pumice). Although the uncertainties of these $f$ values are relatively large, our results support the adequacy of the conventional approach for correction of initial disequilibrium. A recent study published results that apparently show zircon crystallization ages are younger than the eruption age of Bishop Tuff. It seems to be difficult to eliminate these discrepancies, even if the Th/U partitioning and disequilibrium generated during partial melting are taken into account for recalculation of its zircon age. However, magma chamber process and history of Bishop Tuff are too complex to obtain accurate zircon ages by U–Pb method. To overcome this, therefore, the Th–Pb zircon dating method is a key technique for understanding complex, pre-eruptive magma processes, and further efforts to improve its precision and accuracy are desirable.

© 2016 Elsevier B.V. All rights reserved.

## 1. Introduction

Zircon U–series chronometry is a key method for understanding the high-temperature cooling history of magmas (Schmitt, 2011), because it has a relatively high closure temperature (900–1000 °C; Cherniak and Watson, 2001) compared with other chronometers such as $^{40}Ar/^{39}Ar$ sanidine dating (<400 °C; Baadsgaard et al., 1961). Hence, the precise determination of the crystallization age of Quaternary zircons using U–Th–Pb methods is a widely used method of studying magmatic systems (e.g., Bacon et al., 2000; Chamberlain et al., 2014; Oberli et al., 2004; Schmitt, 2011; Schmitt et al., 2003; Simon and Reid, 2005; Simon et al., 2008, 2014). However, when U–Pb dating is applied to young zircons, there has long been concern about the effect of initial disequilibria

* Corresponding author.
*E-mail address:* shuhei.sakata@gakushuin.ac.jp (S. Sakata).

http://dx.doi.org/10.1016/j.quageo.2016.11.002
1871-1014/© 2016 Elsevier B.V. All rights reserved.

associated with intermediate nuclides in the $^{238}U$ or $^{235}U$ decay series (Ludwig, 1977; Mattinson, 1973; Schärer, 1984; Wendt and Carl, 1985). Without correction for the initial disequilibrium, the resulting $^{238}U$–$^{206}Pb$ and $^{235}U$–$^{207}Pb$ ages will deviate systematically from the true ages. For example, in the case of the $^{238}U$ decay series, the contribution of initial disequilibrium can be corrected if the Th/U fractionation between zircon and melt, defined by the Th/U abundance ratio between the zircon and melt (i.e., $(Th/U)_{Zircon}/(Th/U)_{Melt}$), is known (Schärer, 1984). The $(Th/U)_{Zircon}$ value can be directly measured in the zircon, whereas $(Th/U)_{Melt}$ is estimated from the Th/U ratio of the bulk rock (Guillong et al., 2014; Reid et al., 1997; Schmitt et al., 2003), melt inclusions in host rocks (Crowley et al., 2007; Schmitt et al., 2003), or glass in volcanic ash (Matthews et al., 2015). However, it is widely recognized that Th and U could have been heterogeneously distributed in the magma and, moreover, that $(Th/U)_{Melt}$ could change with time due to the crystallization of U–Th-bearing minerals within the melts (Amelin and Zaitsev, 2002). These factors make it difficult to estimate the $(Th/U)_{Melt}$ at the time and site of zircon crystallization.

The $^{238}U$–$^{230}Th$ method is also useful for the determination of crystallization ages of very young minerals (Fukuoka, 1974; Fukuoka and Kigoshi, 1974; Reid et al., 1997). Using this method, zircon ages can be determined by the isochron method through direct measurement of $^{230}Th$. Several studies have successfully dated Quaternary zircons by this method using secondary ionization mass spectrometry (SIMS) or laser ablation, multiple-collector inductively coupled plasma mass spectrometry (LA-MC-ICP-MS) (e.g., Bacon and Lowenstern, 2005; Bernal et al., 2014; Reid et al., 1997). Despite the obvious advantages of the $^{238}U$–$^{230}Th$ method, data from multiple analyses are required to define the isochron, meaning that chronological information cannot be derived solely from a single analysis, unless two point model isochrones (e.g., for zircon–melt) can be constructed. This means that the resulting age represents averaged information from the analyzed crystal(s), and it is difficult to discern the potential multi-stage crystallization history of a single crystal if, for example, Th/U in the melt is variable (Boehnke et al., 2016). In addition, the use of $^{238}U$–$^{230}Th$ dating is limited to ages of <0.4–0.5 Ma, as beyond this the minerals reach secular equilibrium.

In contrast, the $^{232}Th$–$^{208}Pb$ dating method is a potential alternative to U–Pb dating as it does not require correction for the initial disequilibrium effect (Harrison et al., 1995; Oberli et al., 2004). This is because the half-lives of $^{232}Th$ decay series nuclides are significantly shorter than 10 a. The nuclide with the longest half-life is $^{228}Ra$ ($t_{1/2} = 5.75$ a; Mays et al., 1962), meaning that any state of initial disequilibrium is erased on a much shorter time scale than the expected precision of the measured ages. Furthermore, this dating method has a broader range of applications than $^{238}U$–$^{230}Th$ dating. In this study, we use the $^{232}Th$–$^{208}Pb$ method to date three zircon samples separated from Quaternary volcanic rocks and tephras, and we demonstrate the utility of this approach for Quaternary geochronology. We also present and discuss a new approach for constraining the effects of initial disequilibrium in the U decay series based on a comparison between U–Pb and Th–Pb ages.

## 2. Samples

In this study, three zircon samples from volcanic rocks or tephras with relatively high uranium and thorium concentrations were selected for analysis (Table 1), as follows.

(1) A rhyolite (obsidian) from the Wadatouge region in Kirigamine ("Kirigamine Rhyolite"), Nagano, Japan (Oikawa and Nishiki, 2005) contains zircon with high uranium concentrations (ca. 9000 ppm). This rhyolite is a well-known geochemical reference material distributed as JR-1 by the National Institute of Advanced Industrial Science and Technology (AIST), Japan (Imai et al., 1995). It is also used as a reference material for fission-track dating of glass (JAS-G1; Balestrieri et al., 1998). An $^{40}Ar/^{39}Ar$ age of 0.945 ± 0.005 Ma for JAS-G1 glass and a zircon fission-track age of 0.94 ± 0.08 Ma have previously been reported for this rock (Kitada and Wadatsumi, 1995; Sugihara et al., 2009).

(2) Zircons with uranium concentrations of ca. 3000 ppm were separated from the Bishop Tuff, collected from the same outcrop as locality no. 1 (Inyo County, California, USA) described by Izett et al. (1970). Only pumice clasts from the lower part of an air-fall unit at the base of the Bishop Tuff were used, which corresponds to unit F1 described by Hildreth and Wilson (2007). A precisely determined $^{238}U$–$^{206}Pb$ age for Bishop Tuff zircons by Crowley et al. (2007) of 767 ± 1 ka is widely regarded as their crystallization age. However, the Bishop Tuff is a classic zoned deposit and, as such, it is important to relate the ages to the units the samples were collected from. Many studies have documented the heterogeneity of zircons in the Bishop Tuff (e.g., Chamberlain et al., 2014; Reid and Coath, 2000; Reid et al., 2011; Simon and Reid, 2005). Disequilibrium-corrected U–Pb ages for early erupted samples of the Bishop Tuff (766.6 ± 3.2 ka and 774 ± 10 ka for rims and cores of zircon, respectively; Chamberlain et al., 2014) are comparable with those reported by Crowley et al. (2007). In contrast, there are significant differences between published $^{40}Ar/^{39}Ar$ dates of the Bishop Tuff, with dates ranging from ca. 760 to 780 ka, as follows: 758.9 ± 3.6 ka (Sarna-Wojcicki et al., 2000), 767.4 ± 0.4 ka (Rivera et al., 2011), 778.0 ± 7.4 ka (Renne, 2013), and 780 ± 4 ka (Simon et al., 2014). The variability is due to differences in the calibration of the $^{40}Ar/^{39}Ar$ technique and the analytical protocols used in each study (Renne, 2013).

(3) The Toga Pumice is one of our in-house standards, for which both sanidine $^{40}Ar/^{39}Ar$ (0.42 ± 0.01 Ma: Uto et al., 2010) and zircon fission-track ages (0.42 ± 0.08 Ma; Kano et al., 2002) have been reported. The Toga Pumice zircon has an average uranium concentration of ca. 3000 ppm.

The nature of the analyzed samples, sampling localities, and previously reported radiometric ages are summarized in Table 1.

## 3. Analytical method

Zircons were separated from the volcanic rocks and tephras using standard mineral separation techniques. Most zircons from all the samples are euhedral and generally larger than 30 × 100 μm in size. All the zircon grains were mounted on a PFA sheet (0.25 mm thick). Prior to isotopic analysis, the surfaces of the zircon grains were carefully polished using diamond paste (3 and 1 μm). In–situ U–Th–Pb isotopic analyses were carried out using an ICP-MS (AttoM High Resolution-ICP-MS, Nu instruments, Wrexham, UK) coupled to an ArF Excimer laser ablation system (ESI NWR-193, Portland, USA). The laser was operated with a repetition rate of 8 Hz and a spot size of 25–35 μm. A two-volume cell (ESI, Portland, USA) was used throughout the measurements and ablation was carried out in a He atmosphere, utilizing a small volume cell (<1 $cm^3$) to reduce sample washout time. After the ablation cell, the He carrier gas was mixed with Ar gas, and the laser-disintegrated sample particles were delivered to the ICP ion source in a mix of He and Ar. In order to reduce elemental fractionation during

**Table 1**
Details of samples analyzed in this study.

| Sample name | Zircon ID | Approximately concentration | | Sample locality | Reported radiometric ages ± 2σ (Ma) |
|---|---|---|---|---|---|
| | | Th (μg/g) | U (μg/g) | | |
| Kirigamine Rhyolite | KR | ~9000 | ~9000 | Obsidian sample, perlite quarry near Wadatouge Pass, Nagano Prefecture (36°08′ 56″N, 138°08′57″E). Same outcrop as that sampled at Loc. 011124-1A by Sugihara et al. (2009). | 0.945 ± 0.005, GAr[1]<br>0.94 ± 0.08, ZFT[2] |
| Bishop Tuff | BS | ~2000 | ~3000 | Pumice lapilli from 4-m-thick air-fall unit at the base of the Bishop Tuff at the Industrial Minerals quarry (abandoned) 10 km north of Bishop, Inyo County, California (37°27′ N, 118°21′W). Same locality (Locality no.1) as that sampled by Izett et al. (1970). See also Fig. 2 in Izett et al. (1988). | 0.7589 ± 0.0036, SaAr[3]<br>0.7674 ± 0.0004, SaAr[4]<br>0.778 ± 0.0074, SaAr[5]<br>0.780 ± 0.004, SaAr[6]<br>0.767 ± 0.001, ZUPb[7]<br>0.7666 ± 0.0032 from zircon rims, ZUPb[8]<br>0.774 ± 0.010 from zircon cores, ZUPb[8] |
| Toga Pumice | TG | ~4000 | ~3000 | Pumice lapilli from a pumiceus bed of Facies TF4 at north side of Toga Bay, Oga Peninsula, NE Japan. Same locality (Locality no. TOGA-5: 39°57′41″N, 139°42′58″E) as that sampled by Kano et al. (2002). | 0.42 ± 0.08 ZFT[9]<br>0.42 ± 0.02, SaAr[10] |

Abbreviations: GAr, glass Ar/Ar; SaAr, sanidine Ar/Ar; ZFT, zircon fission-track; ZUPb, zircon U-Pb.
[1] Balestrieri et al. (1998), [2] Sugihara et al. (2009), [3] Sarna-Wojcicki et al. (2000), [4] Rivera et al. (2011), [5] Renne (2013), [6] Simon et al. (2014), [7] Crowley et al. (2007), [8] Chamberlain et al. (2014) [9] Kano et al. (2002), [10] Uto et al. (2010).

ablation, a low laser fluence (<2.5 $Jcm^{-2}$) was used throughout this study. A signal-smoothing device was also used (Tunheng and Hirata, 2004).

The LA-ICP-MS operational conditions were optimized by the continuous ablation of zircon 91500 reference material (Wiedenbeck et al., 1995, 2004) and NIST SRM610 glass in order to maximize the signal intensity of $^{238}U$. During LA-ICP-MS analysis, interferences from dioxide ions such as $YbO_2^+$, $LuO_2^+$, and $HfO_2^+$ on Pb isotope masses are extremely small and typically below detection. However, signal intensities on Pb isotopes were also small in this study. Hence, great care was taken to minimize oxide production ($^{232}Th^{16}O^+/^{232}Th^+ < 1\%$). With an ablation spot size of 25 μm and a repetition rate of 8 Hz, typical signal intensities obtained during ablation of NIST SRM610 were $4.4 \times 10^5$ cps for $^{206}Pb$ and $2.0 \times 10^6$ cps for $^{238}U$. Typical gas blank levels were 1300 cps for $^{202}Hg$, 100 cps for $^{206}Pb$, and 80 cps for $^{207}Pb$. For young zircons (<1 Ma), counting statistics can become a major source of analytical error. To maximize the integration times for small Pb signals (e.g., $^{207}Pb$ < 100 cps), U–Pb (i.e., $^{206}Pb/^{238}U$ and $^{207}Pb/^{235}U$ ratio measurements) and Th–Pb age determinations (i.e., $^{208}Pb/^{232}Th$ ratio measurements) were carried out on different zircon grains (i.e., the grains measured for U–Pb and Th–Pb dating were different, but were from the same samples).

There are technical challenges to reliable dating of zircons with very low radiogenic $^{208}Pb/^{232}Th$ by LA-ICP-MS. For zircons <0.5 Ma in age, the $^{208}Pb/^{232}Th$ ratio is < 0.00003 and, therefore, an ion detection system with a wide dynamic range covering 7–8 orders of magnitude is required, particularly for single collector mass spectrometry. In the case of U–Pb or $^{238}U$–$^{230}Th$ dating, measurement of the high $^{238}U$ signal can be avoided by monitoring $^{235}U$ and calculating the signal intensity of $^{238}U$ from an assumed $^{238}U/^{235}U$ ratio (i.e., 137.88; Jaffey et al., 1971). Unfortunately, there is no suitable minor isotope for measurement of Th. To overcome this, we employed new ion counting techniques utilizing an attenuator device, which can reduce the ion counts by a factor of 1/450 (Sakata et al., 2014). Given that the switching time for energizing the attenuator is < 1 ms, only the specific isotopes with high count rates can be monitored with the attenuator even at fast mass scanning. The attenuation device allows the high signal intensity of $^{232}Th$ ($10^8$ cps) to be measured without any deterioration of detector linearity. We monitored $^{238}U$ and $^{232}Th$ by switching the attenuation mode on and off according to the magnitude of their signal intensity.

The possible contribution of common Pb was monitored from the $^{204}Pb$ signal throughout the measurements. However, the $^{204}Pb$ signal has an isobaric interference from $^{204}Hg$; consequently, the contribution of $^{204}Hg$ was determined from the signal intensity of $^{202}Hg$ rationed to the known $^{204}Hg/^{202}Hg$ value of 0.223 (Blum and Bergquist, 2007). With conventional U–Th–Pb age dating using the LA-ICP-MS technique, signal intensities for common Pb contributions to $^{206}Pb$, $^{207}Pb$, and $^{208}Pb$ are calculated from the signal intensity of $^{204}Pb$ by scaling to common Pb ratios of $^{206}Pb/^{204}Pb$, $^{207}Pb/^{204}Pb$, and $^{208}Pb/^{204}Pb$ of 18.700, 15.628 and 38.63, respectively (Stacey and Kramers, 1975). The measured $^{204}Pb$ signals after correction for $^{204}Hg$ were typically <10 cps, showing the corresponding common $^{206}Pb$, $^{207}Pb$, and $^{208}Pb$ signals were similar to the background levels. Given the very low $^{204}Pb$ signal, the propagated uncertainties in the calculated signal intensities for common Pb ($^{206}Pb$, $^{207}Pb$, and $^{208}Pb$) become very large, and thus analyses with significant measured $^{204}Pb$ were not used for the calculation of $f$ factors. As such, no correction for common Pb was made when $^{204}Pb$ signals were below the detection limit. Our LA-ICP-MS technique has detection limits for $^{204}Pb$ (3σ of the $^{204}Pb$ background signal) of 4 and 8 ng/g for a 35 and 25 μm spot size, respectively. This suggests that small amounts of Pb contamination during zircon separation and polishing can cause erroneous U–Th–Pb age determinations. In this study, pre-cleaning of the zircons was carried out by a single pre-ablation shot at each analytical site prior to the actual age determinations (Iizuka and Hirata, 2004).

Elemental fractionation and instrumental mass bias on $^{206}Pb/^{238}U$, $^{208}Pb/^{232}Th$, and $^{207}Pb/^{206}Pb$ ratios were corrected using the measured isotope ratios of the 91500 zircon reference material, without a correction for common Pb. Reference values of $^{206}Pb/^{238}U$ and $^{207}Pb/^{206}Pb$ for 91500 zircon were calculated based on the isotopic data in 'table 1' from Wiedenbeck et al. (1995), whereas the measured $^{208}Pb/^{232}Th$ ratio in 'table 2' of the Wiedenbeck et al. (1995) study was used without common Pb correction. Calculation of measured isotope ratios was conducted using the $^{204}Pb$ method described by Williams (1998), assuming Pb isotope evolution followed a two-stage model (Stacey and Kramers, 1975) and an isotope composition of common Pb at 1065 Ma (i.e., $^{206}Pb/^{204}Pb_{common} = 16.954$, $^{207}Pb/^{204}Pb_{common} = 15.498$, and $^{208}Pb/^{204}Pb_{common} = 36.638$). After calculation of the measured

ratios, a weighted mean for the reference value of 91500 zircon was obtained using ISOPLOT 4.15 (Ludwig, 2003): 0.17928 ± 0.00018 (2 sd; n = 11; $MSWD_W$ = 9.1) for $^{206}Pb/^{238}U$; 0.0540 ± 0.0018 (2 sd; n = 2; MSWD = 3.5) for $^{208}Pb/^{232}Th$; and 0.07556 ± 0.00032 (2 sd; n = 11; MSWD = 13) for $^{207}Pb/^{206}Pb$. External reproducibilities of the Pb/U, Pb/Th, and $^{207}Pb/^{207}Pb$ ratios were determined by repeated analysis of the 91500 zircon. In all analytical sessions involving unknown samples, U–Th–Pb isotope data for Plešovice (337.13 ± 0.37 Ma; Sláma et al., 2008) or OD-3 (33.0 ± 0.1 Ma by SIMS and LA-ICP-MS [Iwano et al., 2013]; 32.853 ± 0.016 Ma by ID-TIMS [Lukács et al., 2015]) zircons were acquired for use as secondary standards. Each laser ablation analysis had a duration of 10 s, which resulted in ablation pits that were ca. 5–8 μm deep. Under these conditions, time-dependent elemental fractionation of Pb/U and Pb/Th was insignificant. Recently, heterogeneous $^{238}U/^{235}U$ values have been reported for terrestrial uranium-bearing minerals (Hiess et al., 2012). The measured variation in $^{238}U/^{235}U$ values of terrestrial zircons is < 1‰, which is much smaller than the uncertainties in the Pb/U measurements achieved in this study; hence, we neglect any possible $^{238}U/^{235}U$ variations and apply the constant value of 137.88 (Jaffey et al., 1971). Therefore, $^{207}Pb/^{235}U$ values were calculated based on the measured $^{206}Pb/^{238}U$ and $^{207}Pb/^{206}Pb$ values, and the assumed $^{238}U/^{235}U$ value.

The overall uncertainties on the Pb/U and Pb/Th age measurements, and $f_{Th/U}$ and $f_{Pa/U}$ values were calculated based on error propagation of: (1) the external reproducibility of the Pb/U, Pb/Th, and $^{207}Pb/^{206}Pb$ measurements determined on 91500 zircon; (2) counting statistics on $^{206}Pb$, $^{207}Pb$, $^{208}Pb$, $^{232}Th$, and $^{238}U$ signals obtained on the unknowns; (3) the $^{230}Th$ decay constant ($\lambda_{230}$ = 9.1705 (±0.0138) × $10^{-6}$ $yr^{-1}$; Cheng et al., 2013); and (4) uncertainties on the reference values of the 91500 zircon. Calculation and propagation of the uncertainties on $f_{Th/U}$ and $f_{Pa/U}$ are discussed in Section 4.2. It should be noted that we did not incorporate uncertainties on the $^{231}Pa$ decay, because it is insignificant compared with the relatively large analytical error on the determination of $f_{Pa/U}$. U–Pb isotopic data for unknowns are summarized in Tables S1 and S2, and for the secondary reference materials are in Tables S3 and S4. The resulting ages for the secondary standards show good agreement with the published values: Plešovice $^{238}U–^{206}Pb$ age = 335.1 ± 2.8 Ma (n = 20; MSWD = 1.12); Plešovice $^{235}U–^{207}Pb$ age = 339.8 ± 3.9 Ma (n = 20; MSWD = 0.78); OD-3 $^{238}U–^{206}Pb$ age = 33.04 ± 0.27 Ma (n = 21; MSWD = 0.74); OD-3 $^{235}U–^{207}Pb$ age = 33.85 ± 0.80 Ma (n = 21; MSWD = 1.4); OD-3 $^{232}Th–^{208}Pb$ age = 33.25 ± 0.40 Ma (n = 17; MSWD = 0.19). All weighted mean values and MSWD values in this study were calculated using Isoplot 4.15 (Ludwig, 2003). Details of the analytical instrumentation and operational settings are summarized in Table 2.

## 4. Results and discussion

### 4.1. Th–Pb and apparent U–Pb ages

Measured $^{232}Th–^{208}Pb$ ages for the Kirigamine Rhyolite, Bishop Tuff, and Toga Pumice are 0.942 ± 0.013 Ma (n = 23; MSWD = 1.3), 0.767 ± 0.015 Ma (n = 31; MSWD = 1.5), and 0.4480 ± 0.0077 Ma (n = 24; MSWD = 0.96), respectively (Fig. 1; Tables S1 and S2). The calculated $^{232}Th–^{208}Pb$ zircon ages for the Kirigamine Rhyolite and Bishop Tuff exhibit good agreement with their $^{40}Ar/^{39}Ar$ sanidine ages considering analytical uncertainties. The consistency of the $^{232}Th–^{208}Pb$ zircon and $^{40}Ar/^{39}Ar$ sanidine ages for the Kirigamine Rhyolite and Bishop Tuff indicates that the residence time for these zircons in their melts was brief (i.e., <0.02 Myr). In contrast, the measured $^{232}Th–^{208}Pb$ zircon age for the Toga Pumice is slightly older than its $^{40}Ar/^{39}Ar$ sanidine age. This can be explained by the higher closure temperature of the $^{232}Th–^{208}Pb$ system in zircon as compared with the $^{40}Ar/^{39}Ar$ system in sanidine, and the possibility of zircons being recycled from a crystal mush or other parts of a long-lived magmatic system (e.g., Schmitt, 2011).

$^{238}U–^{206}Pb$ ages without correction for initial disequilibrium (i.e., assuming that secular equilibrium prevailed during zircon crystallization) are 0.8543 ± 0.0068 Ma (n = 32; MSWD = 0.8) for the Kirigamine Rhyolite, 0.684 ± 0.016 Ma (n = 20; MSWD = 0.4)

**Table 2**
Instrumentation and operational settings.

| | |
|---|---|
| **Laser ablation system** | |
| Instrument | NWR-193 (ESI, Portland, US) |
| Cell type | Two volume cell |
| Laser wave length | 193 nm |
| Pulse duration | 5 ns |
| Fluence | 2.5 J/$cm^2$ |
| Repetition rate | 8 Hz |
| Ablation pit size | 25 μm for Kirigamine Rhyolite and 35 μm for Bishop Tuff, Toga Pumice |
| Sampling mode | Single hole drilling, 1 pre-ablation shots |
| Carrier gas | He gas and Ar make-up gas combined outside ablation cell |
| He gas flow rate | 0.6–0.8 l/min |
| Ar make-up gas flow rate | 0.6–0.9 l/min |
| Ablation duration | 20 s |
| **ICP mass spectrometer** | |
| Instrument | AttoM (Nu Instruments, Wrexham, U.K.) |
| Scan mode | Deflector scan mode |
| Sample introduction | Ablation aerosol only using signal-smoothing device |
| RF power | 1300 W |
| Data reduction | Integration of ion counts per ablation. We skipped signals at first a few seconds for waiting stabilization, and next signals during 7–9 s were integrated for calculation. |
| Monitored mass (dwell time) and number of sweeps | $^{238}U$-$^{206}Pb$ and $^{235}U$-$^{207}Pb$ dating: 202 (1 ms), 204 (1 ms), 206 (1 ms), 207 (1 ms), 232 (1 ms), 238 (1 ms), and 1500 sweeps. Total integration time was 9.0 s.<br>$^{232}Th$-$^{208}Pb$ dating: 202 (0.5 ms), 204 (0.5 ms), 208 (2 ms), 232 (0.6 ms), and 2000 sweeps. Total integration time was 7.2 s. |
| Detector | Unattenuated pulse counting mode for < about 3.0 × $10^6$ cps, attenuated pulse counting mode for > about 3.0 × $10^6$ cps |
| Dead time | 18 ns |
| Formation rate of $^{232}Th^{16}O$ | <1% |

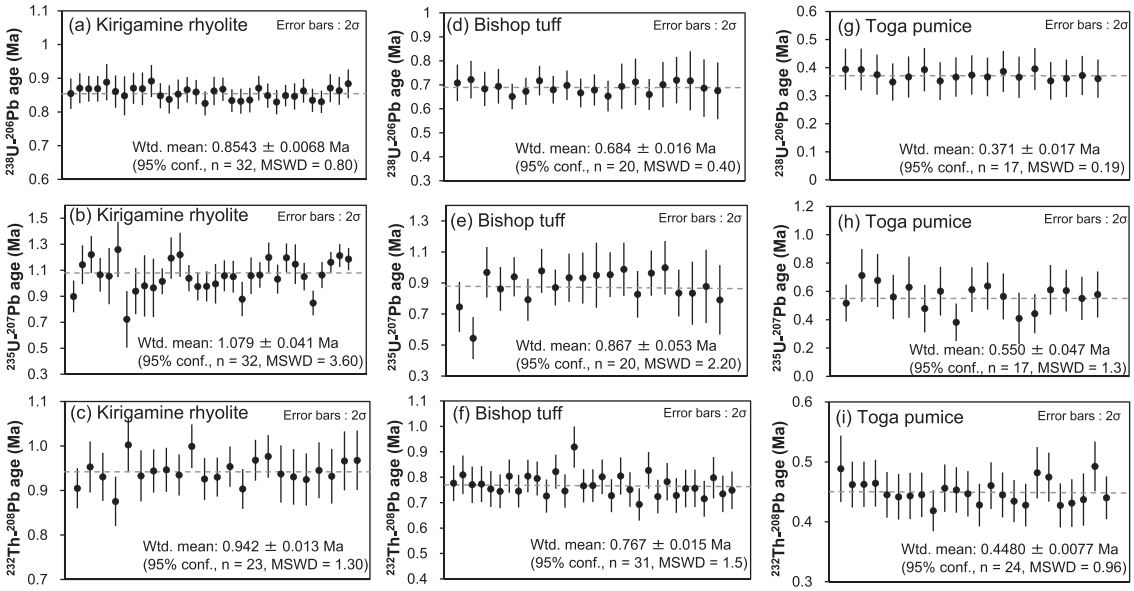


**Fig. 1.** $^{232}$Th–$^{208}$Pb, $^{238}$U–$^{206}$Pb, and $^{235}$U–$^{207}$Pb dating results for the Kirigamine Rhyolite (a–c), Bishop Tuff (d–f), and Toga Pumice (g–i). Note that no correction for initial disequilibrium was applied to the $^{238}$U–$^{206}$Pb and $^{235}$U–$^{207}$Pb ages.

for the Bishop Tuff, and 0.371 ± 0.017 Ma (n = 17; MSWD = 0.19) for the Toga Pumice. The uncorrected $^{235}$U–$^{207}$Pb ages are 1.079 ± 0.041 Ma (n = 32; MSWD = 3.6) for the Kirigamine Rhyolite, 0.867 ± 0.053 Ma (n = 20; MSWD = 2.2) for the Bishop Tuff, and 0.550 ± 0.047 Ma (n = 17; MSWD = 1.3) for the Toga Pumice. The $^{238}$U–$^{206}$Pb and $^{235}$U–$^{207}$Pb ages without correction for initial disequilibrium are significantly younger and older, respectively, than the $^{232}$Th–$^{208}$Pb ages (Fig. 1). This is also evident from the concordia diagrams ($^{206}$Pb/$^{238}$U versus $^{207}$Pb/$^{235}$U; Fig. 2a–c) where all data points for the Kirigamine Rhyolite, Bishop Tuff, and Toga Pumice are systematically displaced to the right of the concordia curve plotted at secular equilibrium. The obvious discrepancy between the measured $^{206}$Pb/$^{238}$U and $^{207}$Pb/$^{235}$U ratios and concordia curves is attributed to the contribution of initial disequilibrium, and deficits and excesses of $^{230}$Th and $^{231}$Pa isotopes, respectively. A modified Tera–Wasserburg ($^{207}$Pb/$^{206}$Pb

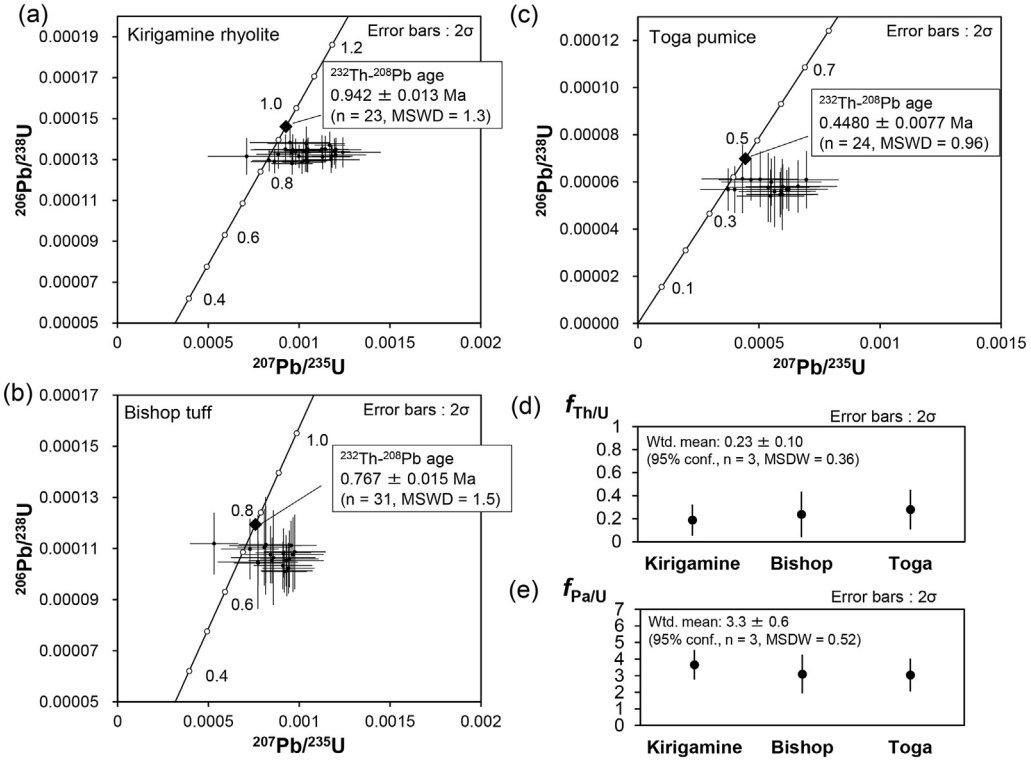


**Fig. 2.** Concordia diagrams for the (a) Kirigamine Rhyolite, (b) Bishop Tuff, and (c) Toga Pumice, and (d and e) resulting $f_{Th/U}$ and $f_{Pa/U}$ values.

versus $^{238}U/^{206}Pb$) concordia diagram has been proposed that can account for initial disequilibrium of $^{234}U$, $^{231}Pa$, $^{230}Th$, and $^{226}Ra$ (Richards et al., 1998; Wendt and Carl, 1985). However, for the case of U–Th–Pb dating of zircon, we now present simplified corrections for disequilibrium and demonstrate their viability.

### 4.2. Simplified disequilibrium corrections

In a state of radioactive secular equilibrium, the product of radiogenic nuclides ($N_i$) and their decay constants ($\lambda_i$) for all decay series nuclides is constant (i.e., $N_i\lambda_i$ = constant). Initial disequilibrium results from preferential redistribution of decay series nuclides during crystallization of minerals, including zircon (Fukuoka, 1974; Fukuoka and Kigoshi, 1974; Rubatto and Hermann, 2007). Due to this initial disequilibrium (i.e., $N_i\lambda_i \neq$ constant), the growth rates of radiogenic $^{206}Pb$ and $^{207}Pb$ isotopes deviate from those under secular equilibrium. In the case of the $^{238}U$ decay series, elemental fractionation of $^{230}Th$ from $^{238}U$ during zircon crystallization in a melt can cause the initial disequilibrium. The same is true for the $^{235}U$ decay series, where preferential incorporation of $^{231}Pa$ relative to $^{235}U$ in zircon can cause initial disequilibrium (e.g., Schmitt, 2007, 2011). The contribution of other nuclides is negligible, because of the shorter half-lives of the other decay series nuclides. The magnitude of the initial disequilibrium in the $^{238}U$–$^{206}Pb$ and $^{235}U$–$^{207}Pb$ decay systems can be estimated from the ratio of the distribution coefficients for Th/U ($D^{Th}_{Zircon/Melt}/D^{U}_{Zircon/Melt}$) and Pa/U ($D^{Pa}_{Zircon/Melt}/D^{U}_{Zircon/Melt}$), respectively. Hence, the correction factors for the initial disequilibrium on $^{238}U$–$^{206}Pb$ and $^{235}U$–$^{207}Pb$ decay series can be defined as follows:

$$f_{Th/U} = \frac{D^{Th}_{Zircon/Melt}}{D^{U}_{Zircon/Melt}} = \frac{(Th/U)_{Zircon}}{(Th/U)_{Melt}} \quad (1)$$

$$f_{Pa/U} = \frac{D^{Pa}_{Zircon/Melt}}{D^{U}_{Zircon/Melt}} = \frac{(Pa/U)_{Zircon}}{(Pa/U)_{Melt}}. \quad (2)$$

Given that the distribution coefficients ($D_{Zircon/Melt}$) can vary depending on the chemical composition, oxygen fugacity, pressure or temperature of the melts (Blundy and Wood, 2003; Luo and Ayers, 2009; Rubatto and Hermann, 2007) and the crystallization rate (Trail, 2014), $f_{Th/U}$ and $f_{Pa/U}$ values can deviate from unity. This suggests that initial equilibrium is generally not expected to exist for magmatic zircons. Ludwig (1977) and Wendt and Carl (1985) formalized the contribution of initial radioactive-daughter disequilibrium to U–Pb decay systems. This was followed by a practical correction technique for initial disequilibrium using $f_{Th/U}$ values (Schärer, 1984), which is, however, oversimplified. Using the correction technique of Schärer (1984), the resulting U–Pb dates are only sufficiently accurate for zircons >0.5 Ma. However, these disequilibrium effects on young zircon ages (<0.5 Ma) must be carefully corrected for. To overcome this problem, equations for the correction of initial disequilibrium are derived here by simplifying the original equations of Wendt and Carl (1985), and by reasonably assuming that: (a) the state of secular equilibrium for the U–Th–Pb decay series was achieved in the melt from which the zircons crystallized (e.g., Condomines and Sigmarsson, 1993); (b) the $^{234}U/^{238}U$ ratio did not change due to zircon crystallization; (c) the initial Pb ($^{204}Pb$, $^{206}Pb$, $^{207}Pb$, and $^{208}Pb$) in the zircon was negligible (i.e., $Pb_0 = 0$); and (d) the effect of initial disequilibrium on $^{226}Ra$ ($t_{1/2}$ = 1600 a) and other nuclides with shorter half-lives can be ignored.

Under these conditions, the following relationships between $^{238}U$, $^{234}U$, and $^{230}Th$ activities are valid:

$$^{238}U^{Crystl.}_{Melt}\lambda_{238} = {}^{234}U^{Crystl.}_{Melt}\lambda_{234} = {}^{230}Th^{Crystl.}_{Melt}\lambda_{230} \quad (3)$$

where $^{234}U$, $^{238}U$, and $^{230}Th$ denote the number of atoms and $\lambda_m$ (m = 238, 234 and 230) are the decay constants for $^{238}U$, $^{234}U$, and $^{230}Th$, respectively, and *Crystl.* represents the timing of the zircon crystallization. For the $^{238}U$ and $^{234}U$ nuclides, it is reasonable to assume that radioactive equilibrium is maintained, as isotope fractionation between $^{234}U$ and $^{238}U$ during high temperature crystallization is negligible and, hence, the ratio of their distribution coefficients ($D^{234\text{-}U}/D^{238\text{-}U}$) will be unity. Thus, we derive the following relationship between the number of nuclides ($^{234}U$ and $^{238}U$) and their decay constants:

$$^{238}U^{Crystl.}_{Zircon}\lambda_{238} = {}^{234}U^{Crystl.}_{Zircon}\lambda_{234} \quad (4)$$

Given that Pb is highly incompatible in zircon, we assume that the content of initial Pb (non-radiogenic Pb) is zero:

$$^{206}Pb^{Initial}_{Zircon} = 0 \quad (5)$$

The temporal changes in the $^{206}Pb$ and $^{230}Th$ nuclides are expressed as follows:

$$\frac{d^{230}Th_{Zircon}}{dt} = {}^{234}U_{Zircon}\lambda_{234} - {}^{230}Th_{Zircon}\lambda_{230} \quad (6)$$

and

$$\frac{d^{206}Pb^{*}_{Zircon}}{dt} = {}^{230}Th_{Zircon}\lambda_{230}, \quad (7)$$

where $Pb^*$ represents radiogenic Pb. Using reasonable approximations ($\lambda_{230} - \lambda_{238} \sim \lambda_{230}$; $\lambda_{231} - \lambda_{235} \sim \lambda_{231}$), the ingrowth of the $^{206}Pb/^{238}U$ ratio with time can be calculated as follows:

$$\left(\frac{^{206}Pb^{*}_{Zircon}}{^{238}U_{Zircon}}\right) = \left(e^{\lambda_{238}t} - 1\right) + \frac{\lambda_{238}}{\lambda_{230}}\left(f_{Th/U} - 1\right)\left(1 - e^{-\lambda_{230}t}\right)e^{\lambda_{238}t} \quad (8)$$

In an identical fashion, the equation for the ingrowth of $^{207}Pb/^{235}U$ can be derived:

$$\left(\frac{^{207}Pb^{*}_{Zircon}}{^{235}U_{Zircon}}\right) = \left(e^{\lambda_{235}t} - 1\right) + \frac{\lambda_{235}}{\lambda_{231}}\left(f_{Pa/U} - 1\right)\left(1 - e^{-\lambda_{231}t}\right)e^{\lambda_{235}t} \quad (9)$$

These formulae are the basis for the correction of $^{238}U$–$^{206}Pb$ and $^{235}U$–$^{207}Pb$ ages from measured $(^{206}Pb/^{238}U)_{Zircon}$ and $(^{207}Pb/^{235}U)_{Zircon}$ and two correction factors ($f_{Th/U}$ and $f_{Pa/U}$) defined in Equations (8) and (9). The correction factors $f_{Th/U}$ and $f_{Pa/U}$ can be represented as follows:

$$f_{Th/U} = \frac{\lambda_{230}\left\{R_{206/238} - \left(e^{\lambda_{238}t} - 1\right)\right\}}{\lambda_{238}\left(1 - e^{-\lambda_{230}t}\right)e^{\lambda_{238}t}} + 1 \quad (10)$$

$$f_{Pa/U} = \frac{\lambda_{231}\left\{R_{207/235} - \left(e^{\lambda_{235}t} - 1\right)\right\}}{\lambda_{235}\left(1 - e^{-\lambda_{231}t}\right)e^{\lambda_{235}t}} + 1 \quad (11)$$

where $R_{206/238}$ and $R_{207/235}$ represent $^{206}Pb/^{238}U$ and $^{207}Pb/^{235}U$ ratios in the zircon, respectively. Equations (8)–(11) are mathematically equivalent to those published by Wendt and Carl (1985) with the exception that we neglect the initial disequilibrium of

$^{234}$U and $^{226}$Ra. Propagation of uncertainties on $f_{Th/U}$ and $f_{Pa/U}$ can be calculated using the following equations:

$$\sigma^2 f_{Th/U} = \left(\frac{\lambda_{230}}{\lambda_{238}\left(1-e^{-\lambda_{230}t}\right)e^{\lambda_{238}t}}\right)^2 \sigma^2 R_{206/238} + \left(\frac{\lambda_{230}\left[-\lambda_{238}e^{\lambda_{238}t}\left(1-e^{-\lambda_{230}t}\right)-\left(R_{206/238}+1-e^{\lambda_{238}t}\right)\left\{\left(-\lambda_{230}e^{-\lambda_{230}t}\right)+\left(1-e^{-\lambda_{230}t}\right)\lambda_{238}\right\}\right]}{\lambda_{238}\left(1-e^{-\lambda_{230}t}\right)^2 e^{\lambda_{238}t}}\right)^2 \sigma^2 t + \left(\frac{\left(R_{206/238}-e^{\lambda_{238}t}+1\right)\left(1-e^{-\lambda_{230}t}-\lambda_{230}te^{-\lambda_{230}t}\right)}{\lambda_{238}\left(1-e^{-\lambda_{230}t}\right)^2 e^{\lambda_{238}t}}\right)^2 \sigma^2 \lambda_{230} \quad (12)$$

$$\sigma^2 f_{Pa/U} = \left(\frac{\lambda_{231}}{\lambda_{235}\left(1-e^{-\lambda_{231}t}\right)e^{\lambda_{235}t}}\right)^2 \sigma^2 R_{207/235} + \left(\frac{\lambda_{231}\left[-\lambda_{235}e^{\lambda_{235}t}\left(1-e^{-\lambda_{231}t}\right)-\left(R_{207/235}+1-e^{\lambda_{235}t}\right)\left\{\left(-\lambda_{231}e^{-\lambda_{231}t}\right)+\left(1-e^{-\lambda_{231}t}\right)\lambda_{235}\right\}\right]}{\lambda_{235}\left(1-e^{-\lambda_{231}t}\right)^2 e^{\lambda_{235}t}}\right)^2 \sigma^2 t + \left(\frac{\left(R_{207/235}-e^{\lambda_{235}t}+1\right)\left(1-e^{-\lambda_{231}t}-\lambda_{231}te^{-\lambda_{231}t}\right)}{\lambda_{235}\left(1-e^{-\lambda_{231}t}\right)^2 e^{\lambda_{235}t}}\right)^2 \sigma^2 \lambda_{231} \quad (13)$$

In Equations (12) and (13), $\sigma R_{206/238}$ and $\sigma R_{207/235}$ are the uncertainties on $(^{206}Pb/^{238}U)_{Zircon}$ and $(^{207}Pb/^{235}U)_{Zircon}$, respectively. Similarly, uncertainties on the age (t), and $^{230}$Th and $^{231}$Pa decay constants are represented as $\sigma t$ and $\sigma\lambda$, and are propagated as a source of error, whereas errors on the $^{238}$U and $^{235}$U decay constants are ignored. In the case of LA-ICP-MS zircon dating, the analytical uncertainties are typically a few percent, and the contribution to the final error from the error of the $^{230}$Th decay constant ($\lambda_{230} = 9.1705\ (\pm 0.00138) \times 10^{-6}\ yr^{-1}$; Cheng et al., 2013) is trivial compared with the analytical uncertainties. Hence, the uncertainty on $\lambda_{230}$ can be ignored (i.e., $\sigma\lambda_{230} = 0$) in LA-ICP-MS studies.

Fig. 3 illustrates the growth curve for the $(^{206}Pb/^{238}U)_{Zircon}$ ratio calculated as a function of $f_{Th/U}$ values. For comparison, the growth curves for $(^{206}Pb/^{238}U)_{Zircon}$ proposed by Schärer (1984) and the conventional growth curves without any correction for initial disequilibrium (i.e., $^{206}Pb/^{238}U = e^{\lambda t} - 1$) are also shown. The magnitude of the systematic difference in the measured age (t) with and without correction of initial disequilibrium is ~100 ka (e.g., $f_{Th/U} = 0.1$); thus, reliable $f$ -values are required for the accurate correction of initial disequilibrium. It is impossible to calculate $f_{Th/U}$ and $f_{Pa/U}$ from direct comparison of measured $^{206}Pb/^{238}U$ and $^{207}Pb/^{235}U$ ratios and time (t) defined by zircon fission track (FT) or $^{40}Ar/^{39}Ar$ ages for the same volcanic event. This would be erroneous because U–Pb, FT, and $^{40}Ar/^{39}Ar$ ages have markedly different closure temperatures: ca. 250 °C for zircon FT dating (Hurford, 1986; Tagami et al., 1996), <400 °C for $^{40}Ar/^{39}Ar$ dating (e.g., sanidine; Baadsgaard et al., 1961), and 900–1000 °C for zircon U–Th–Pb ages (Cherniak and Watson, 2001). Moreover, zircon commonly crystallizes significantly before eruption (e.g., Simon et al., 2008). To overcome this, we have determined empirical $f_{Th/U}$ and $f_{Pa/U}$ factors based on a comparison of the $^{206}Pb/^{238}U$ and $^{207}Pb/^{235}U$ ratios with the measured $^{232}Th–^{208}Pb$ ages for the Kirigamine Rhyolite, Bishop Tuff, and Toga Pumice (e.g., Oberli et al., 2004). These solutions for $f$ are based on the fact that the $^{232}Th–^{208}Pb$ decay series is not significantly affected by initial disequilibrium effects because the half-lives of $^{232}$Th -decay series nuclides are <5.75 a ($^{228}$Ra; Mays et al., 1962), meaning that any disequilibrium is erased on a much shorter time scale than the corresponding analytical uncertainties on $^{232}Th–^{208}Pb$ ages.

### 4.3. $f$ value determination

In this study, $f_{Th/U}$ and $f_{Pa/U}$ values in Equations (10) and (11) were calculated from the measured $^{206}Pb/^{238}U$ and $^{207}Pb/^{235}U$ ratios and the $^{232}Th–^{208}Pb$ ages. Fig. 2d and e illustrate the resulting $f_{Th/U}$ and $f_{Pa/U}$ values obtained from our three zircon samples. The resulting correction factors are $f_{Th/U} = 0.19 \pm 0.14$ and $f_{Pa/U} = 3.66 \pm 0.89$ for the Kirigamine Rhyolite, $f_{Th/U} = 0.24 \pm 0.20$ and $f_{Pa/U} = 3.1 \pm 1.2$ for the Bishop Tuff, and $f_{Th/U} = 0.28 \pm 0.17$ and $f_{Pa/U} = 3.04 \pm 0.99$ for the Toga Pumice (2 sd absolute; Fig. 2d and e; Table S2). Amongst our three studied zircon samples, the Bishop Tuff has been the subject of the most previous studies to constrain the degree of initial disequilibrium (i.e., determine $f_{Th/U}$). Crowley et al. (2007) determined a precise $^{238}U–^{206}Pb$ ages for Bishop Tuff zircons by ID-TIMS, using 2.81 ± 0.32 (2σ) as the Th/U value in the melt for estimating $f_{Th/U}$. This value was derived from data in Anderson et al. (2000) who analyzed of melt inclusions in quartz phenocrysts that were shown to be uniform throughout the entire

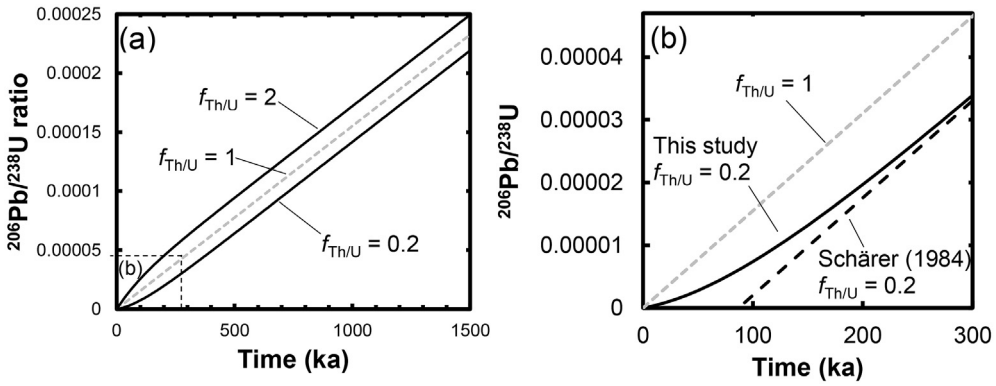


**Fig. 3.** $^{206}Pb/^{238}U$ growth curves in zircon calculated using Equation (8).

Bishop Tuff eruptive cycle. The data in Crowley et al. (2007) can be inverted to calculate a $f_{Th/U}$ value for Bishop Tuff zircon on Equations (10) and (12). This yields $f_{Th/U} = 0.1949 \pm 0.0078$ ($2\sigma$; n = 19; MSWD = 2.0). Alternatively, Th/U melt values of the Long Valley volcano system, which is the source of the Bishop Tuff (Hildreth and Wilson, 2007; Simon et al., 2014), combined with Th/U zircon data from Crowley et al. (2007), yield $f_{Th/U}$ values between 0.11 and 0.21. The $f_{Th/U}$ value estimated in this study ($f_{Th/U} = 0.24 \pm 0.20$) is consistent with these previous studies considering the uncertainties. However, the magnitude of the uncertainty is too large to rigorously evaluate differences between the approaches for estimating $f_{Th/U}$; i.e., from Th/U melt values, or combination of Th–Pb ages and radiogenic Pb/U in the zircon.

Unfortunately, there are no previous studies that allow us to constrain $f_{Th/U}$ in zircons from the Kirigamine Rhyolite and Toga Pumice. Typically, reported $f_{Th/U}$ values of zircons that crystallized from silicic magmas range from ca. 0.15 to 0.25 (e.g., Charlier and Zellmer, 2000; Farley et al., 2002; Guillong et al., 2014; Schmitt, 2011; Schmitt et al., 2003; Simon et al., 2009). Experimentally determined distribution coefficients for Th and U ($D^{Th}$ and $D^{U}$) in a zircon–melt system have been determined, and from these, $f_{Th/U}$ (i.e., $D^{Th}/D^{U}$) can be calculated to be ca. 0.16 to 0.25 at 750–800 °C (Rubatto and Hermann, 2007; Watson and Harrison, 1983). Compared with these accepted values for $f_{Th/U}$, the values obtained in our study ($f_{Th/U} = 0.19 \pm 0.14$ for the Kirigamine Rhyolite; $f_{Th/U} = 0.28 \pm 0.17$ for the Toga Pumice) have similar or slightly higher values which overlap within uncertainty. The precision of $f_{Th/U}$ achieved in this study is insufficient for identifying the best approach to quantifying the degree of initial $^{230}Th$ disequilibrium, but the results indicate that estimation of $f_{Th/U}$ using whole-rock or melt inclusion chemistry is consistent with our independent approach of using Th–Pb ages.

There have only been limited investigations of the magnitude of Pa/U partitioning in the zircon–melt system (i.e., $f_{Pa/U}$). Although direct experimental constrains on $f_{Pa/U}$ are lacking, Schmitt (2007) measured the $^{231}Pa/^{235}U$ ratio and calculated initial $^{231}Pa/^{235}U$ in natural zircons from the continental rift Salton Buttes rhyolite. Schmitt (2007) estimated that the $f_{Pa/U}$ value of zircon is ca. 0.9 to 2.2. Subsequently, Schmitt (2011) determined the initial $^{231}Pa/^{235}U$ ratio in zircon crystals from the Late Pleistocene China Hat rhyolite by measuring $^{230}Th/^{238}U$ and $^{231}Pa/^{235}U$ ratios by SIMS. Given that the initial $^{231}Pa/^{235}U$ ratio in the melt of the zircon was also measured by glass analysis (Heumann, 2004), a $f_{Pa/U}$ value of ca. 3.8 could be calculated (Schmitt, 2011). The $f_{Pa/U}$ values determined for natural zircon samples in our study (ca. 3.0 to 3.7) are in good agreement with those of Schmitt (2011) considering the uncertainties. These values agree with those estimated from ID-TIMS zircon data where disequilibrium corrected $^{206}Pb/^{238}U$ ages were compared to $^{207}Pb/^{235}U$ ages (Rioux et al., 2015).

However, we have to deal with an urgent problem associated with the age of Bishop Tuff, if our estimation of Th/U and Pa/U partitioning in zircon-melt system supports the conventional approach for correction of initial disequilibrium.

### 4.4. Is the 767 ka zircon date the age of the Bishop Tuff?

Recent studies of the age of the Bishop Tuff have led to controversy regarding the differences between the eruption age determined by $^{40}Ar/^{39}Ar$ methods on sanidine and the crystallization age determined by U–Pb methods on zircon. The weighted mean zircon U–Pb age of 767 ± 1 ka ($2\sigma$; n = 17/19) determined by Crowley et al. (2007) has been widely accepted and is consistent with the slightly younger 759 ± 4 ka ($2\sigma$; n = 70) $^{40}Ar/^{39}Ar$ eruption age of Sarna-Wojcicki et al. (2000). However, this $^{40}Ar/^{39}Ar$ age changes significantly depending on the calibration strategy (Channell et al., 2010; Renne, 2013; Renne et al., 1998, 2011; Rivera et al., 2011; Simon et al., 2014). Simon et al. (2014) precisely determined an eruption age of 780 ± 4 ka ($2\sigma$) using the calibration method of Renne et al. (2011), which agrees with that of Sarna-Wojcicki et al. (2000) recalculated using the same calibration, and shows good reproducibility from a large number of analyses (n = 120) of multiple samples from the Bishop Tuff. Therefore, we consider that an age of 780 ± 4 ka ($2\sigma$) is one of reliable determinations of the eruption age of the Bishop Tuff. However, if one accepts this eruption age, then the younger zircon crystallization age (767 ± 1 ka; $2\sigma$) determined by Crowley et al. (2007) becomes problematic. Simon et al. (2014) suggested that this was because the estimation of the Th/U ratio of the host melt by Crowley et al. (2007) was erroneous and, as a result, the correction for initial disequilibrium on $^{230}Th$ was incorrect. Crowley et al. (2007) adopted a Th/U melt value of 2.81 ± 0.32 ($2\sigma$), whereas Simon et al. (2014) suggested that this value is higher. For example, if the average Th/U melt value of 3.5 estimated by Hildreth and Wilson (2007) or a value of 4.5 determined from late-erupting pumice is used instead, then the age of Crowley et al. (2007) can be recalculated to be 771–775 ka. Nevertheless, this recalculated age still appears to be younger than the eruption age. Here, we would like to explore another explanation for this inconsistency in these ages and assess if the scenario is realistic.

Many recent studies have highlighted that the typical intervals between major silicic eruptions are, surprisingly, longer than the periods in which the melts can remain in a molten state (Druitt et al., 2012; Reid, 2008; Reid and Coath, 2000; Simon and Reid, 2005; Simon et al., 2008, 2009), whereas Tierney et al. (2016)

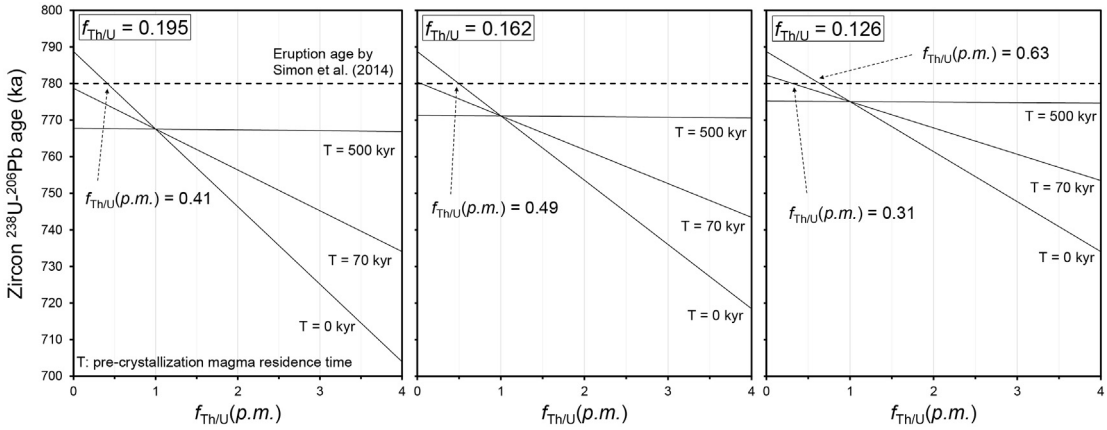


**Fig. 4.** Recalculated zircon $^{238}U$–$^{206}Pb$ ages of Bishop Tuff when the Th/U partitioning and disequilibrium generated during partial melting are taken into account. For calculation, isotopic data of zircon grains in Crowley et al. (2007) is used. Here, $f_{Th/U}(p.m.)$ and $f_{Th/U}$ are the fractionation factor of Th/U at the time of partial melting or zircon crystallization, respectively, T is the pre-crystallization magma residence time (i.e., the time between partial melting and zircon crystallization). Three $f_{Th/U}$ values are calculated by procedures described in text.

show that long melt presence (>400 kyr) is possible under realistic condition of magma fluxes. Hence, melt disequilibrium (or equilibrium) of Bishop Tuff should be a valid concern. If a state of secular equilibrium was not reached in the melt of the Bishop Tuff, then assumption (a) in Section 4.2 is no longer correct. In this case, the equation for the $^{238}U$–$^{206}Pb$ age can be modified using distribution coefficients for Th–U in solid–initial melt at the time of partial melting (i.e., $D^{Th}_{Solid/Initial\ Melt}$ and $D^{U}_{Solid/Initial\ Melt}$), and zircon–melt (i.e., $D^{Th}_{Zircon/Melt}$ and $D^{U}_{Zircon/Melt}$) systems as follows:

$$\left(\frac{^{206}Pb^{*}_{Zircon}}{^{238}U_{Zircon}}\right) = e^{\lambda_{238}t} - 1 + \frac{\lambda_{238}}{\lambda_{230}}\left[f_{Th/U}\left\{1 + e^{(\lambda_{238}-\lambda_{230})T}\left(f_{Th/U}(p.m.) - 1\right)\right\} - 1\right]\left(1 - e^{-\lambda_{230}t}\right)e^{\lambda_{238}t} \quad (14)$$

$$f_{Th/U}(p.m.) = \frac{D^{Th}_{Solid/Initial\ Melt}}{D^{U}_{Solid/Initial\ Melt}} = \frac{(Th/U)_{Solid}}{(Th/U)_{Initial\ Melt}} \quad (15)$$

where $f_{Th/U}(p.m.)$ and $f_{Th/U}$ are the fractionation factor of Th/U at the time of partial melting or zircon crystallization, respectively, T is the pre-crystallization magma residence time (i.e., the time between partial melting and zircon crystallization), and t is the zircon crystallization age. $(Th/U)_{Solid}$ and $(Th/U)_{Initial\ Melt}$ are the Th/U values of the magma source, such as continental crust, depleted mantle, or older magmatic intrusions, and the initial melt at the time of partial melting, respectively. Equation (14) shows that the disequilibrium-corrected age becomes older as T becomes shorter. Furthermore, the corrected age is also older if the fractionation factor for Th/U in the solid–initial melt system ($f_{Th/U}(p.m.)$) is less than unity. It is difficult to precisely determine the pre-crystallization magma residence time of the melt of Bishop Tuff, but we can estimate that the value is < 70 kyr, if we accept a proposed model of magma chamber history of Long Valley caldera by Simon et al. (2014). Hence, we can calculate the amount of melt disequilibrium ($f_{Th/U}(p.m.)$) required to bring eruption and crystallization ages to concordance. In this discussion, three different cases are considered. In first scenario, the magnitude of disequilibrium in zircon–melt system ($f_{Th/U}$) is fixed to be weighted average of $f_{Th/U}$ values calculated from isotopic data in Crowley et al. (2007) and 2.81 ± 0.32 (2σ) as the melt Th/U value (Anderson et al., 2000): $f_{Th/U}$ = 0.195. In second and third scenarios, $f_{Th/U}$ values are calculated to be 0.162 and 0.126 using the melt Th/U value of 3.5 (Hildreth and Wilson, 2007) and 4.5 from late-erupting pumice (Simon et al., 2014), respectively. To bring zircon crystallization ages (t) recalculated using these parameters (i.e., $f_{Th/U}$, T) to be older than the eruption age of Simon et al. (2014), the melt disequilibrium values ($f_{Th/U}(p.m.)$) corresponding to three $f_{Th/U}$ values must be smaller than 0.41, 0.49, or 0.63, respectively, even if the pre-crystallization magma residence time (T) is assumed to be zero (Fig. 4). Here, Bishop Tuff can be classified into rhyolitic rock (e.g., Hildreth and Wilson, 2007), and rhyolites that are sufficiently young to directly measure U-series isotopes are typically close to equilibrium (Boehnke et al., 2016; Condomines and Sigmarsson, 1993), unless the Th concentration of melt is relatively low (<2 ppm, Condomines and Sigmarsson, 1993). It would be unrealistic to consider that a strong melt disequilibrium ($f_{Th/U}(p.m.)$ <0.41, 0.49, or 0.63) existed at the timing of partial melting because the melt Th concentration of Bishop Tuff is relatively high (>10 ppm, Simon et al., 2014).

However, in general, the processes involving the intrusion of silicic magmas are more complex than the simplified model assumed above. For example, the Long Valley caldera has experienced multiple intrusions of silicic magma from 2500 to 100 ka (Bailey et al., 1976; Heumann and Davies, 1997; Metz and Bailey, 1993; Simon et al., 2014) and, therefore, robust estimation of $f_{Th/U}(p.m.)$ and T is difficult. Therefore, our approach using zircon Th–Pb ages has some important advantages over other methods for correcting for initial disequilibrium. This is because no assumptions need to be made regarding elemental fractionation in solid–initial melt and zircon–melt systems or complex magma chamber processes. We have determined a Th–Pb age for Bishop Tuff zircons of 767 ± 15 ka (n = 31; MSWD = 1.5), which is within uncertainties of the eruption ages by Sarna-Wojcicki et al. (2000) and Simon et al. (2014). Although it is difficult to confirm which eruption age is reliable from the point of view of our Th–Pb age of Bishop Tuff zircons, this method still provides a critical constraint on the timing of zircon crystallization. To determine Th–Pb ages more precisely using LA–ICP–MS methods, several technical advances remain to be achieved. These include development of reliable secondary reference materials of young age for $^{208}Pb/^{232}Th$ measurements, enhanced instrument sensitivity, and improvement of common Pb correction. As such, we do not consider our Th–Pb age as the best constraint on the crystallization age of Bishop Tuff zircons, given the large uncertainty associated with it. However, it is clear that

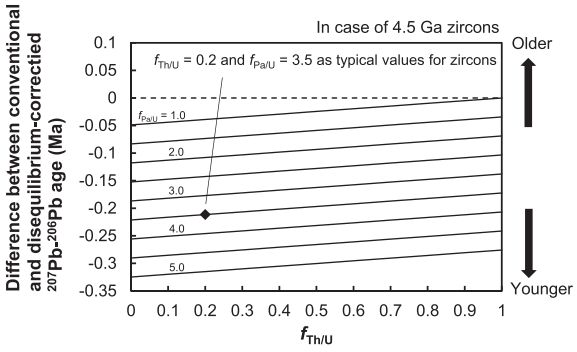


**Fig. 5.** Systematic errors in $^{207}Pb/^{206}Pb$ ages dependent on the initial disequilibria of $^{230}Th$ and $^{231}Pa$ in the case of a zircon with an age of 4.5 Ga. The difference between the conventional (assuming secular equilibrium) and disequilibrium-corrected ages was calculated as follows: (corrected $^{207}Pb/^{206}Pb$ age) − (conventional $^{207}Pb/^{206}Pb$ age).

Th–Pb dating can contribute to the investigation of complex magma chamber processes and, therefore, developing improved techniques for Th–Pb dating is an important area for future research.

### 4.5. Effect of initial disequilibrium on $^{207}Pb/^{206}Pb$ ages

A failure to account for initial disequilibrium causes an apparent offset in $^{238}U$–$^{206}Pb$ and $^{235}U$–$^{207}Pb$ ages. This implies that initial disequilibrium can cause systematic age errors for ancient zircons where precisions of <0.1 Myr are sought on measured ages. Moreover, this is also the case for $^{207}Pb/^{206}Pb$ ages, which are widely used to define ages for older zircons (>500 Ma). We have evaluated the effect of initial disequilibrium for a hypothetical zircon that is 4.5 Ga in age (Fig. 5). Using typical correction factors for silicic magmas ($f_{Th} = 0.2$ and $f_{Pa} = 3.5$), the difference between $^{207}Pb/^{206}Pb$ ages calculated with and without correction for initial disequilibrium is ca. 0.2 Myr (Fig. 5). This is equivalent to systematic errors in $^{207}Pb/^{206}Pb$ ages resulting from documented variations in $^{238}U/^{235}U$ (Hiess et al., 2012). The timescale for planetary accretion and differentiation in the early Solar System is < 3 Myr (e.g., Allégre et al., 1995; Göpel et al., 1994), and this also highlights the importance of assessing systematic errors resulting from initial disequilibrium when high-resolution chronology based on $^{207}Pb/^{206}Pb$ ages is required to investigate planetary processes.

## 5. Concluding remarks

We have determined $^{238}U$–$^{206}Pb$, $^{235}U$–$^{207}Pb$, and $^{232}Th$–$^{208}Pb$ ages on three Quaternary zircon samples by LA-ICP-MS, providing novel insights into methods used to constrain initial disequilibrium effects on U–Pb and Pb–Pb dating. The main outcomes of our study are as follows.

(1) $^{232}Th$–$^{208}Pb$ ages for the Kirigamine Rhyolite, Bishop Tuff, and Toga Pumice are determined to be 0.942 ± 0.013, 0.767 ± 0.015, and 0.4480 ± 0.0077 Ma, respectively.
(2) We propose a simplified correction model for initial disequilibrium effects on $^{230}Th$ and $^{231}Pa$ in U–Pb zircon dating based on the mathematical framework of Wendt and Carl (1985).
(3) Through comparison of $^{238}U$–$^{206}Pb$ (or $^{235}U$–$^{207}Pb$) and $^{232}Th$–$^{208}Pb$ zircon ages, correction factors for initial disequilibrium are calculated to be 0.19–0.28 for $f_{Th/U}$ and 3.0–3.7 for $f_{Pa/U}$, which are consistent with those determined previously using Th/U or Pa/U values in zircons and their melts.
(4) Discrepancies in the eruption and zircon crystallization ages of the Bishop Tuff is difficult to be reconciled by taking into account a disequilibrium correction model using Th/U partitioning in zircon–melt and solid–initial melt systems. Although our newly obtained Th–Pb zircon age of 767 ± 15 ka is not precise enough to strongly constrain the sanidine $^{40}Ar/^{39}Ar$ eruption age of Bishop Tuff, Th–Pb dating can be a key method to determine the timing of zircon crystallization in Quaternary timescales.
(5) Systematic errors in $^{207}Pb/^{206}Pb$ zircon ages arising from initial disequilibrium effects are ca. 0.2 Myr for 4.5 Ga zircon, assuming typical Th/U and Pa/U partitioning in a zircon–melt system. This may be significant for early Solar System time scales, highlighting the importance of considering and correcting for initial disequilibrium when high-resolution chronologies are required.

In summary, zircon Th–Pb dating is not only an important tool for age determinations, but also a novel approach to investigating Th/U or Pa/U partitioning in magmatic systems.

## Acknowledgements

A critical review by Axel Schmitt greatly improved this manuscript, and editorial handling by David Richards is gratefully acknowledged. We thank Albrecht von Quadt (ETH Zürich, Switzerland), Yuji Orihashi (Earthquake Research Institute, The University of Tokyo, Japan), Tsuyoshi Iizuka (The University of Tokyo, Japan), Kenshi Maki (Akita University, Japan), Robert Nesbitt (Instituto Espanol de Oceanografia, School of Ocean and Earth Science, Spain), Yumiko Watanabe (Kyoto University, Japan), and Yugo Danhara (Kyoto Fission-Track Co. Ltd.) for scientific advice and technical support. All the zircon samples were kindly provided by Kyoto Fission-Track Co. Ltd. (Kyoto, Japan). This work was supported by a Grant-in-Aid for Scientific Research (A26247094) to TH from the Ministry of Education, Culture, Sports, Science and Technology, Japan.

## Appendix A. Supplementary data

Supplementary data related to this article can be found at http://dx.doi.org/10.1016/j.quageo.2016.11.002.

## References

Allégre, C.J., Manhés, G., Göpel, C., 1995. The age of the Earth. Geochim. Cosmochim. Acta 59, 1445–1456.
Amelin, Y., Zaitsev, A.N., 2002. Precise geochronology of phoscorites and carbonatites: the critical role of U-series disequilibrium in age interpretations. Geochim. Cosmochim. Acta 66, 2399–2419.
Anderson, F.T., Davis, A.M., Lu, F., 2000. Evolution of Bishop Tuff rhyolitic magma based on melt and magnetite inclusions and zoned phenocrysts. J. Petrol 41, 449–473.
Baadsgaard, H., Lipson, J., Folinsbee, R.E., 1961. The leakage of radiogenic argon from sanidine. Geochim. Cosmochim. Acta 25, 147–157.
Bacon, C.R., Persing, H.M., Wooden, J.L., Ireland, T.R., 2000. Late Pleistocene granodiorite beneath Crater Lake caldera, Oregon, dated by ion microprobe. Geology 28, 467–470.
Bacon, C.R., Lowenstern, J.B., 2005. Late Pleistocene granodiorite source for recycled zircon and phenocrysts in rhyodacite lava at Crater Lake. Or. Earth Planet. Sci. Lett. 233, 277–293.
Bailey, R.A., Dalrymple, G.B., Lanphere, M.A., 1976. Volcanism, structure, and geochronology of Long-Valley Caldera, Mono-County, California. J. Geophys. Res. 81, 725–744.
Balestrieri, M.L., Bigazzi, G., Bouška, V., Labrin, E., Hadler, J.C., Kitada, N., Osorio, A., Poupeau, G., Wadatsumi, K., Zúñiga, A., 1998. Potential glass age standards for fission-track dating: an overview. In: Van den haute, P., De Corte, F. (Eds.), Advances in Fission-track Geochronology. Kluwer Academic Publishers,

Dordrecht, pp. 47–66.
Bernal, J.P., Solari, L.A., Gómez-Tuena, A., Ortega-Obregón, C., Mori, L., Vega-González, M., Espinosa-Arbeláez, D.G., 2014. *In-situ* $^{230}$Th/U dating of Quaternary zircons using LA-MCICPMS. Quat. Geochronol. 23, 46–55.
Blum, J.D., Bergquist, D.A., 2007. Reporting of variations in the natural isotopic composition of mercury. Anal. Bioanal. Chem. 388, 353–359.
Blundy, J., Wood, B., 2003. Mineral–melt partitioning of uranium, thorium and their daughters. Rev. Mineral. Geochem 52, 59–123.
Boehnke, P., Barboni, M., Bell, E.A., 2016. Zircon U/Th model ages in the presence of melt heterogeneity. Quat. Geochronol. http://dx.doi.org/10.1016/j.quageo.2016.03.005.
Chamberlain, K.J., Wilson, C.J.N., Wooden, J.L., Charlier, B.L.A., Ireland, T.R., 2014. New perspectives on the Bishop Tuff from zircon textures, ages and trace elements. J. Petrol. 55, 395–426.
Channell, J.E.T., Hodell, D.A., Singer, B.S., Xuan, C., 2010. Reconciling astrochronological and $^{40}$Ar/$^{39}$Ar ages for the Matuyama–Brunhes boundary and late Matuyama Chron. Geochem. Geophys. Geosyst. 11, 1525–2027. http://dx.doi.org/10.1029/2010GC003203.
Charlier, B., Zellmer, G., 2000. Some remarks on U–Th mineral ages from igneous rocks with prolonged crystallization histories. Earth Planet. Sci. Lett. 183, 457–469.
Cheng, H., Edwards, R.L., Shen, C.C., Polyak, V.J., Asmerom, Y., Woodhead, J., Hellstrom, J., Wang, Y., Kong, X., Spötl, C., Wang, X., Alexander Jr., E.C., 2013. Improvements in $^{230}$Th dating, $^{230}$Th and $^{234}$U half-life values, and U–Th isotopic measurements by multi-collector inductively coupled plasma mass spectrometry. Earth Planet. Sci. Lett. 371–372, 82–91.
Cherniak, D.J., Watson, E.B., 2001. Pb diffusion in zircon. Chem. Geol. 172, 5–24.
Condomines, M., Sigmarsson, O., 1993. Why are so many arc magmas close to $^{238}$U–$^{230}$Th radioactive equilibrium? Geochim. Cosmochim. Acta 57, 4491–4497.
Crowley, J.L., Schoene, B., Bowring, S.A., 2007. U–Pb dating of zircon in the Bishop Tuff at the millennial scale. Geology 35, 1123–1126.
Druitt, T.H., Costa, F., Deloule, E., Dungan, M., Scaillet, B., 2012. Decadal to monthly timescales of magma transfer and reservoir growth at a caldera volcano. Nature 482, 77–80.
Farley, K.A., Kohn, B.P., Pillans, B., 2002. The effects of secular disequilibrium on (U–Th)/He systematics and dating of Quaternary volcanic zircon and apatite. Earth Planet. Sci. Lett. 201, 117–125.
Fukuoka, T., 1974. Ionium dating of acidic volcanic rocks. Geochem. J. 8, 109–116.
Fukuoka, T., Kigoshi, K., 1974. Discordant Io-ages and the uranium and thorium distribution between zircon and host rocks. Geochem. J. 8, 117–122.
Göpel, C., Manhés, G., Allégre, C.J., 1994. U–Pb systematics of phosphates from equilibrated ordinary chondrites. Earth Planet. Sci. Lett. 121, 153–171.
Guillong, M., von Quadt, A., Sakata, S., Peytcheva, I., Bachmann, O., 2014. LA-ICP-MS Pb–U dating of young zircons from the Kos-Nisyros volcanic centre, SE Aegean arc. J. Anal. At. Spectrom. 29, 963–970.
Harrison, T.M., McKeegan, K.D., LeFort, P., 1995. Detection of inherited monazite in the Manaslu leucogranite by $^{208}$Pb/$^{232}$Th ion microprobe dating: crystallization age and tectonic implications. Earth Planet. Sci. Lett. 133, 271–282.
Heumann, A., 2004. Timescales of evolved magma generation at Blackfoot Lava Field, SE Idaho, USA. Presented at Int. Assoc. Volcanol. Chem. Earth's Inter. 2004 Gen. Assembly, Nov. 14–19, Pucon, Chile.
Heumann, A., Davies, G.R., 1997. Isotopic and chemical evolution of the post-caldera rhyolitic system at Long Valley, California. J. Petrol. 38, 1661–1678.
Hiess, J., Condon, D.J., McLean, N., Noble, S.R., 2012. $^{238}$U/$^{235}$U Systematics in terrestrial uranium-bearing minerals. Science 335, 1610–1614.
Hildreth, W., Wilson, C.J.N., 2007. Compositional zoning of the Bishop Tuff. J. Petrol. 48, 951–999. http://dx.doi.org/10.1093/petrology/egm007.
Hurford, A.J., 1986. Cooling and uplift patterns in the Lepontine Alps South Central Switzerland and an age of vertical movement on the Insubric fault line. Contrib. Mineral. Petrol. 92, 413–427.
Iizuka, T., Hirata, T., 2004. Simultaneous determinations of U–Pb and REE abundances for zircons using ArF excimer laser ablation-ICPMS. Geochem. J. 38, 229–241.
Imai, N., Terashima, S., Itoh, S., Ando, A., 1995. 1994 compilation of analytical data for minor and trace elements in seventeen GSJ geochemical reference samples "Igneous Rock Series". Geostand. Newsl. 19, 135–213.
Iwano, H., Orihashi, Y., Hirata, T., Ogasawara, M., Danhara, T., Horie, K., Hasebe, N., Sueoka, S., Tamura, A., Hayasaka, Y., Katsube, A., Ito, H., Tani, K., Kimura, J., Chang, Q., Kouchi, Y., Haruta, Y., Yamamoto, K., 2013. An inter-laboratory evaluation of OD-3 zircon for use as a secondary U–Pb dating standard. Isl. Arc 22, 382–394.
Izett, G.A., Obradovich, J.D., Mehnert, H.H., 1988. The Bishop Ash Bed (Middle Pleistocene) and Some Older (Pliocene and Pleistocene) Chemically and Mineralogically Similar Ash Beds in California, Nevada, and Utah, U.S. Geological Survey Bulletin 1675. United States Government Printing Office, Washington.
Izett, G.A., Wilcox, R.E., Powers, H.A., Desborough, G.A., 1970. The Bishop ash bed, a Pleistocene marker bed in the Western United States. Quat. Res. 1, 121–132.
Jaffey, A.H., Flynn, K.F., Glendenin, L.E., Bentleyt, W.C., Essling, A.M., 1971. Precision measurement of half-lives and specific activities of $^{235}$U and $^{238}$U. Phys. Rev. C 4, 1889–1906.
Kano, K., Ohguchi, T., Hayashi, S., Uto, K., Danhara, T., 2002. Toga Volcano: an alkali rhyolite tuff-ring in the western end of Oga Peninsula, NE Japan. Volcano 47, 373–396.
Kitada, N., Wadatsumi, K., 1995. Proposal for a glass age standard "JAS-G1". Bull. Liaison Inf. IUGS Subcomm. Geochronol. 13, 23–27.
Lukács, R., Harangi, S., Bachmann, O., Guillong, M., Danišik, M., Buret, Y., von Quadt, A., Dunkl, I., Fodor, L., Sliwinski, J., Soós, I., Szepesi, J., 2015. Zircon geochronology and geochemistry to constrain the youngest eruption events and magma evolution of the Mid-Miocene ignimbrite flare-up in the Pannonian Basin, eastern central Europe. Contrib. Mineral. Petrol. 170, 52.
Ludwig, K.R., 1977. Effect of initial radioactive-daughter disequilibrium on U–Pb isotope apparent ages of young minerals. J. Res. U.S. Geol. Surv. 5, 663–667.
Ludwig, K.R., 2003. Isoplot/Ex Ver. 3.00, a Geochronological Tool Kit for Microsoft Excel. Berkeley, California, Berkeley Geochronology Center Special Publication 4, 71.
Luo, Y., Ayers, J.C., 2009. Experimental measurements of zircon/melt trace-element partition coefficients. Geochim. Cosmochim. Acta 73, 3656–3679.
Matthews, N.E., Vazquez, J.A., Calvert, A.T., 2015. Age of the Lava Creek supereruption and magma chamber assembly from combined $^{40}$Ar/$^{39}$Ar and U–Pb dating of sanidine and zircon crystals. Geochem. Geophys. Geosyst. 16, 2508–2528.
Mattinson, J.M., 1973. Anomalous Isotopic Composition of Lead in Young Zircons. In: Carnegie Institution of Washington Year Book, vol. 72, pp. 613–616.
Mays, C.W., Atherton, D.R., Lloyd, R.D., Lucas, H.F., Stover, B.J., Bruenger, F.W., 1962. The Half-period of Ra 228 (Mesothorium). Utah Univ. Report, COO-225, 92–105.
Metz, J., Bailey, R.A., 1993. Geologic Map of Glass Mountain, Mono County, California. In: U.S. Geological Survey Miscellaneous Investigations Series I–1995.
Oberli, F., Meier, M., Berger, A., Rosenberg, C.L., Gieré, R., 2004. U–Th–Pb and $^{230}$Th/$^{238}$U disequilibrium isotope systematics: precise accessory mineral chronology and melt evolution tracing in the Alpine Bergell intrusion. Geochim. Cosmochim. Acta 68, 2543–2560.
Oikawa, T., Nishiki, K., 2005. K–Ar ages of the lavas from Kirigamine Volcano, central Japan. Volcano 50, 143–148.
Reid, M.R., 2008. How long does it take to supersize an eruption? Elements 4, 23–28.
Reid, M.R., Coath, C.D., 2000. In situ U–Pb ages of zircons from the Bishop Tuff: no evidence for long crystal residence times. Geology 28, 443–446.
Reid, M.R., Coath, C.D., Harrison, T.M., McKeegan, K.D., 1997. Prolonged residence times for the youngest rhyolites associated with Long Valley Caldera: $^{230}$Th–$^{238}$U ion microprobe dating of young zircons. Earth Planet. Sci. Lett. 150, 27–39.
Reid, M.R., Vazquez, J.A., Schmitt, A.K., 2011. Zircon-scale insights into the history of a Supervolcano, Bishop Tuff, Long Valley, California, with implicationsfor the Ti-in-zircon geothermometer. Contrib. Mineral. Petrol. 161, 293–311.
Renne, P.R., 2013. Some footnotes to the optimization-based calibration of the $^{40}$Ar/$^{39}$Ar system. In: Jourdan, F., Mark, D.F., Verati, C. (Eds.), Advances in $^{40}$Ar/$^{39}$Ar Dating: from Archeology to Planetary Science, Geological Society, London, Special Publications 378. http://dx.doi.org/10.1144/SP378.17.
Renne, P.R., Swisher, C.C., Deino, A.L., Karner, D.B., Owens, T.L., DePaolo, D.J., 1998. Intercalibration of standards, absolute ages and uncertainties in $^{40}$Ar/$^{39}$Ar dating. Chem. Geol. 145, 117–152.
Renne, P.R., Balco, G., Ludwig, K.R., Mundil, R., Min, K.W., 2011. Response to the comment by W.H. Schwarz et al., on "Joint determination of $^{40}$K decay constants and $^{40}$Ar*/$^{40}$K for the Fish Canyon sanidine standard, and improved accuracy for $^{40}$Ar/$^{39}$Ar geochronology" by P.R. Renne et al. (2010). Geochim. Cosmochim. Acta 75, 5097–5100.
Richards, D.A., Bottrell, S.H., Cliff, R.A., Ströhle, K., Rowe, P.J., 1998. U–Pb dating of a speleothem of Quaternary age. Geochim. Cosmochim. Acta 62, 3683–3688.
Rioux, M., Bowring, S., Cheadle, M., John, B., 2015. Evidence for initial excess $^{231}$Pa in mid-ocean ridge zircons. Chem. Geol. 397, 143–156.
Rivera, T.A., Storey, M., Zeeden, C., Hilgen, F.J., Kuiper, K., 2011. A refined astronomically calibrated $^{40}$Ar/$^{39}$Ar age for Fish Canyon sanidine. Earth Planet. Sci. Lett. 311, 420–426.
Rubatto, D., Hermann, J., 2007. Experimental zircon/melt and zircon/garnet trace element partitioning and implications for the geochronology of crustal rocks. Chem. Geol. 241, 38–61.
Sakata, S., Hattori, K., Iwano, H., Yokoyama, T.D., Danhara, T., Hirata, T., 2014. Determination of U–Pb ages for young zircons using a laser ablation-ICP-mass spectrometry coupled with attenuator ion detection device. Geostand. Geoanal. Res. 38, 409–420. http://dx.doi.org/10.1111/j.1751-908X.2014.00320.x.
Sarna-Wojcicki, A.M., Pringle, M.S., Wijbrans, J., 2000. New $^{40}$Ar/$^{39}$Ar age of the Bishop Tuff from multiple sites and sediment rate calibration for the Matuyama–Brunhes boundary. J. Geophys. Res. 105, 431–443.
Schärer, U., 1984. The effect of initial $^{230}$Th disequilibrium on young U–Pb ages: the Makalu case, Himalaya. Earth Planet. Sci. Lett. 67, 191–204.
Schmitt, A.K., 2007. Ion microprobe analysis of ($^{231}$Pa)/($^{235}$U) and an appraisal of protactinium partitioning in igneous zircon. Am. Mineral. 92, 691–694.
Schmitt, A.K., 2011. Uranium series accessory crystal dating of magmatic processes. Ann. Rev. Earth Pl. Sci. 39, 321–349.
Schmitt, A.K., Grove, M., Harrison, M., Lovera, O., Hulen, J., Walters, M., 2003. The Geysers - Cobb Mountain Magma System, California (Part 1): U–Pb zircon ages of volcanic rocks, conditions of zircon crystallization and magma residence times. Geochim. Cosmochim. Acta 67, 3423–3442.
Simon, J.I., Reid, M.R., 2005. The pace of rhyolite differentiation and storage in an 'archetypical' silicic magma system, Long Valley, California. Earth Planet. Sci. Lett. 235, 123–140.
Simon, J.I., Renne, P.R., Mundil, R., 2008. Implications of pre-eruptive magmatic histories of zircons for U–Pb geochronology of silicic extrusions. Earth Planet. Sci. Lett. 266, 182–194.

Simon, J.I., Vazquez, J.A., Renne, P.R., Schmitt, A.K., Bacon, C.R., Reid, M.R., 2009. Accessory mineral U–Th–Pb ages and $^{40}Ar/^{39}Ar$ eruption chronology, and their bearing on rhyolitic magma evolution in the Pleistocene Coso volcanic field, California. Contrib. Mineral. Petrol. 158, 421–446.

Simon, J.I., Weis, D., DePaolo, D.J., Renne, P.R., Mundil, R., Schmitt, A.K., 2014. Assimilation of preexisting Pleistocene intrusions at Long Valley by periodic magma recharge accelerates rhyolite generation: rethinking the remelting model. Contrib. Mineral. Petrol. 167, 1–34.

Sláma, J., Košler, J., Condon, D.J., Crowley, J.L., Gerdes, A., Hanchar, J.M., Horstwood, M.S.A., Morris, G.A., Nasdala, L., Norberg, N., Schaltegger, U., Schoene, B., Tubrett, M.N., Whitehouse, M.J., 2008. Plešovice zircon — A new natural reference material for U–Pb and Hf isotopic microanalysis. Chem. Geol. 249, 1–35.

Stacey, J.S., Kramers, J.D., 1975. Approximation of terrestrial lead isotope evolution by a two-stage model. Earth Planet. Sci. Lett. 26, 207–221.

Sugihara, S., Nagai, M., Shibata, T., Danhara, T., Iwano, H., 2009. Petrographic and geochemical study and fission-track dating of obsidian from the Kirigamine and Kitayatsugatake areas in the central part of Japan: the fundamental research for sourcing of obsidian artifacts. Sundai Hist. Rev. 136, 57–109.

Tagami, T., Carter, A., Hurford, A.J., 1996. Natural long-term annealing of the zircon fission-track system in Vienna Basin deep borehole samples: constraints upon the partial annealing zone and closure temperature. Chem. Geol. 130, 147–157.

Tierney, C.R., Schmitt, A.K., Lovera, O.M., de Silva, S.L., 2016. Voluminous plutonism during volcanic quiescence revealed by thermochemical modeling of zircon. Geology 44 (8), 683–686.

Trail, D., 2014. Heterogeneous distribution of trace elements in zircon. In: Abstract Goldschmidt Conference, Sacramento. http://goldschmidt.info/2014/uploads/abstracts/finalPDFs/2510.pdf.

Tunheng, A., Hirata, T., 2004. Development of signal smoothing device for precise elemental analysis using laser ablation-ICP-mass spectrometry. J. Anal. At. Spectrom. 19, 932–934.

Uto, K., Kano, K., Ishizuka, O., 2010. Laser-fusion $^{40}Ar/^{39}Ar$ dating on sanidine phenocrysts from Toga pumice, Toga Volcano, Oga Peninsula, northeast Japan. Volcano 55, 201–206.

Watson, E.B., Harrison, T.M., 1983. Zircon saturation revisited: temperature and composition effects in a variety of crustal magma types. Earth Planet. Sci. Lett. 64, 295–304.

Wendt, I., Carl, C., 1985. U/Pb dating of discordant 0.1 Ma old secondary U minerals. Earth Planet. Sci. Lett. 73, 278–284.

Wiedenbeck, M., Alle, P., Corfu, F., Griffin, W.L., Meier, M., Oberli, F., van Quadt, A., Roddick, J.C., Spiegel, W., 1995. Three natural zircon standards for U–Th–Pb, Lu–Hf, trace element and REE analyses. Geostand. Newslett. 19, 1–23.

Wiedenbeck, M., Hanchar, J.M., Peck, W.H., Sylvester, P., Valley, J., Whitehouse, M., Kronz, A., Morishita, Y., Nasdala, L., Fiebig, J., Franchi, I., Girard, J.P., Greenwood, R.C., Hinton, R., Kita, N., Mason, P.R.D., Norman, M., Ogasawara, M., Piccoli, P.M., Rhede, D., Satoh, H., Schulz-Dobrick, D., Skår, O., Spicuzza, M.J., Terada, K., Tindle, A., Togashi, S., Vennemann, T., Xie, Q., Zheng, Y.F., 2004. Further characterisation of the 91500 zircon crystal. Geostand. Geoanal. Res. 28, 9–39.

Williams, I.S., 1998. U–Th–Pb geochronology by ion microprobe. In: McKibben, M.A., Shanks III, W.C., Ridley, W.I. (Eds.), Applications of Microanalytical Techniques to Understanding Mineralizing Processes, Reviews in Economic Geology, vol. 7, pp. 1–35.